International Journal of Thermal Sciences 84 (2014) 158–163

Contents lists available at ScienceDirect

International Journal of Thermal Sciences

journal homepage: www.elsevier.com/locate/ijts

Onset of Marangoni convection in low viscosity silicon oil inside a heated capillary tube

Cosimo Buffone [a, *], Anselmo Cecere [b], Raffaele Savino [b], Romain Rioboo [c], Joël De Coninck [c], Stefan Van Vaerenbergh [a]

[a] Microgravity Research Centre, Université Libre de Bruxelles, Av. F. Roosevelt 50, 1050 Bruxelles, Belgium
[b] Dipartimento di Ingegneria Industriale (DII) – Sezione Aerospaziale, Università degli studi di Napoli Federico II, Piazzale Tecchio, 80, 80125 Napoli, Italy
[c] Laboratorie de Physique des Surfaces et Interface, Université de Mons, Belgium

ARTICLE INFO

Article history:
Received 12 September 2013
Received in revised form
15 May 2014
Accepted 21 May 2014
Available online

Keywords:
Marangoni convection
InfraRed thermography
Low viscosity silicon oil

ABSTRACT

In the present experimental investigation the onset of Marangoni convection inside a heated capillary tube filled with low viscosity silicon oil is presented and discussed. The 1 cSt viscosity silicon oil used evaporates spontaneously at ambient temperature. The evaporation of silicon oil inside the 1 mm internal diameter tube is not uniform, being larger near the meniscus triple line region than in the centre; this creates gradients of temperatures (which have been measured by InfraRed thermography) and therefore of surface tension. For the unheated tubes this gradient of surface tension is found to be not big enough to set a convection motion (Marangoni convection) which was reported by one of the present authors in previous studies using alcohols. With increasing power supplied to the tube by an electric heater, the Marangoni convection sets in and strengthens at increasing powers till the pinned meniscus detaches from the tube mouth and recedes inside the capillary.

1. Introduction

Phase change (evaporation, condensation and boiling) is key to many industrial applications such as condensers, heat pipes [1], and combustion. The last decade has seen miniaturization of components such as cars condenser because of the higher performances found at small scale [2]. At small scale (typically below few millimetres) surface tension plays an important role and it is believed to enhance the heat and mass transfer because of the thinning of the micro-region where most of the phase change takes place [3]. Surface tension is important to many other industrial applications such a glass manufacture [4], crystal growth [5], and welding [6].

An overview of different research advancements on the subject, with particular attention to the potential technological applications of Marangoni convection and instabilities, including solidification and crystal growth, bubbles and drops dynamics, heat and mass transfer, multiphase flows processes, can be found in Ref. [7].

One of the present authors has reported in numerous publications the self-induced evaporation of volatile liquids inside capillary tubes [8–11]. The thermocapillary convection observed was characterised by the use of μ-Particle Image Velocimetry. Evaporation rates were also measured as well as the tracer particle spinning frequency. It was found that small tube sizes strongly enhance the evaporation flux and the tracers spinning frequency (which is a measure of vorticity) [8]. The competition between surface tension and gravity forces observed [9], produces an important distortion of the Marangoni toroidal vortex which has important potential implications in crystal growth. In Buffone et al. [10] the authors report instabilities in a horizontally oriented 600 μm tube filled with ethanol; instabilities were found in the Marangoni vortex, in the meniscus position at the tube mouth and in the meniscus temperature. InfraRed temperature measurements were performed in Buffone and Sefiane [11], for different capillary tube sizes and different alcohols; it was concluded that small tube sizes and more volatile liquids create larger temperature deeps at the meniscus micro-region where most of the evaporation takes place.

Dhavaleswarapu et al. [12] reproduced the results of Buffone and Sefiane [8] and Buffone et al. [9] by analysing 5 different tube sizes ranging from 75 to 1,575 μm using μ-Particle Image Velocimetry. They found that the evaporation rate and flux scale parabolically and hyperbolically respectively instead of linearly as in Buffone and Sefiane [8]; the vorticity scales hyperbolically with the

* Corresponding author. Tel.: +32 2650 3029; fax: +32 2650 3126.
E-mail addresses: cbuffone@ulb.ac.be, cosimobuffone@hotmail.com (C. Buffone).

http://dx.doi.org/10.1016/j.ijthermalsci.2014.05.020
1290-0729/

tube diameter in contrast with the linear relationship of Buffone et al. [9]. Chamarthy et al. [13] reported μ-Particle Image Velocimetry measurements of horizontally oriented capillary tubes with ethanol as working fluid. They found distortion of the flow field which they attributed to the action of gravity; interestingly they reported that there is no distortion of the flow pattern for capillary sizes of 75 μm. This is a very interesting finding with important repercussions in industrial and lab applications such as crystal growth.

InfraRed temperature measurements have been recently conducted to map the temperature distribution on the liquid of a heated sessile water droplet [14]. The authors found a non-uniform temperature distribution along the droplet surface with lower temperatures at the contact line compared to the droplet top. The evaporation mechanism in sessile drops is similar to the meniscus interface inside a tube investigated in the present work.

Transient Marangoni convection in pendant evaporating drops of different liquids have been investigated both numerically and experimentally, using a *laser sheet* illumination system and a video camera for tracer particles visualization and infrared temperature measurements in Refs. [15,16]. More recently, infrared visualization of thermal motion inside evaporating sessile drops of ethanol, methanol and FC-72 onto a heated surface has been investigated [17].

It is well known in literature dealing with Marangoni flows that a surface tension gradient exceeding a threshold value corresponding to a critical Marangoni number lead to an onset of convective flow, of the type of the Benard–Marangoni instability that was originally observed on a thin liquid layer. Such variations of the surface tension can arise naturally due to the dependence of the surface tension on the temperature field and on the concentration of dissolved species in binary or multicomponent liquid mixtures. For single-component evaporative systems, the onset of Marangoni convection is generally driven by temperature gradients. In this case thermal energy is removed from the liquid resulting in local change in the temperature and thus also in the surface tension.

Onset of Marangoni convection in evaporating sessile or pending drops has received attention in literature [18–20]. Despite numerous studies about Marangoni flows, there are very few of them conducted for the meniscus in microscale channels or tubes, which is a topic of interest in various heat transfer and microfluidic applications. For instance in Ref. [21] a numerical study is conducted on a flat meniscus considering an evaporative heat flux, with the initial meniscus temperature uniform. In this case the temperature gradients induced by the liquid evaporation may exceed a threshold value and thermocapillary convection is establishing. Knowledge of the critical surface tension difference provides guidance for design of a microfluidic device [21]. In a similar paper [22], the authors study the same problem and investigate the onset of the convective instability when the channel size or the temperature gradient are beyond certain values. The threshold Marangoni number for the instability turns out to be dependent also on the Biot number.

In the present work low viscosity silicon oil (which evaporates at ambient temperature) has been used inside a borosilicate tube of 1 mm ID positioned horizontally. The tube is heated by an electric heater made of a wire wrapped around the tube. The threshold temperature difference at the meniscus interface is induced by heating the system with the electric heater and only when the power settings become large enough the on-set of Marangoni convection is established. The convection pattern has been monitored by measuring the tracer particles spinning frequency (a measure of vorticity); InfraRed temperature measurements have also been performed along the meniscus interface at the tube mouth.

2. Experimental apparatus

The tube is a 1 mm ID (1.32 mm OD) made of borosilicate glass and is 100 mm long. The tube is positioned horizontally on a three-dimensional microstage with a 5 μm accuracy. The silicon oil made by Sigma–Aldrich has a viscosity of 1 cSt and it is therefore slightly volatile. The physical properties of the silicon oil used are reported in Table 1. The emissivity of the silicone oil has been set to 0.9, according to previous literature studies [16]. A number of tests were carried out in Savino and Fico [16] showing that the silicon oils employed are not transparent at the thermocamera wavelength, and therefore the observed temperature is the surface temperature with very little contribution of the liquid immediately beneath the surface. The tube was filled with silicon oil positioning one meniscus at the tube mouth (pinned meniscus) and leaving the second meniscus receding inside the tube while mass is being lost at the pinned meniscus. A small electric wire has been wrapped (7 turns not uniformly separated) around the tube to produce a heater. The heater is positioned at 5 mm from the tube mouth and is 3 mm in length. An electric power supply with fine tuning knobs has been used to deliver small power increments to the heater.

Two kinds of experiments have been performed in the present study. In the first experiment nylon tracer particles of average size 15 μm have been used to seed the silicon oil near the tube mouth. Fig. 1 is a photograph of the experimental set-up showing a microscope, a CCD camera of 752 × 480 pixels, and a computer with specialised "home-made" software used to track the particles and determine their spinning frequency as a function of the applied power. A power supply has been used to power the electric heater shown in the inset of Fig. 1.

The gravitational forces arising from the mismatch between tracers and fluid density are evaluated with the following formula (coming from Stokes's drag law) [23]:

$$U_{zP} - U_z = d_P^2 \frac{\rho_P - \rho}{18\mu} g$$

where, U_{zP} and U_z are the particle and fluid vertical velocity components respectively, d_P is the particle diameter, ρ_P (1000 kg/m3) and ρ (820 kg/m3) are the particles and fluid density respectively, μ (0.00082 Pa s) is the fluid dynamic viscosity and g is the gravitational acceleration. The aforementioned formula for the present case leads to:

$$U_{zP} - U_z \cong 4.8\ 10^{-4}\ \mathrm{m\ s^{-1}}$$

whereas the average particles velocity measured along the meniscus ($(U_{zP} \cong 5\ 10^{-4}\ \mathrm{m\ s^{-1}})$) for the highest heater power setting of 1.08 W is slightly higher. Therefore, we cannot strictly assume that the particles are neutrally buoyant. Smaller or less heavy particles would generate more accurate results.

In the second experiment InfraRed (IR) thermography has been employed to measure the temperature distribution on diametrical

Table 1
Thermophysical properties of 1 cSt silicone oil at 25 °C.

Density (kg/m^3)	Surface tension (mN/m)	Surface tension derivative (mN/m/K)	Specific heat (J/kg/K)	Thermal conductivity (W/m/K)	Dynamic viscosity (Pa s)	Thermal expansion coefficient (1/K)
820	16.9	0.06	2000	0.1	0.82 10^{-3}	1.3 10^{-3}

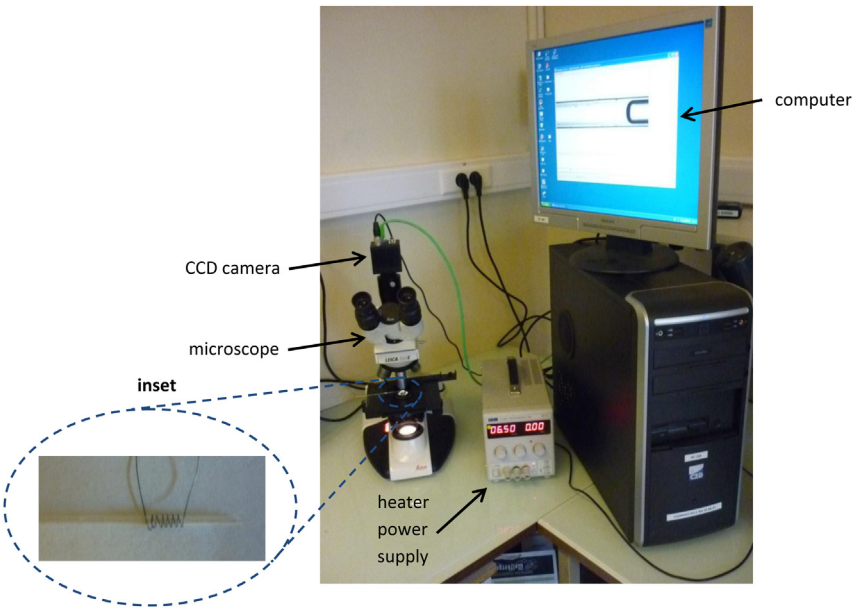

Fig. 1. Experimental apparatus for tracking tracer particles. In the inset a close-up view of the tube showing the coils of the electric heater.

sections along the meniscus interface. The disposition of the IR camera is reported in Fig. 2, which is the same as used during a previous investigation (Buffone and Sefiane [11]). The IR camera of the present study is a Flir SC5000 with 320 × 256 pixel resolution, a 20 mK sensitivity and a 1.5 °C accuracy at full scale for temperature up to 150 °C. The camera is equipped with an Indium Antimonide (InSb) focal plane array detector and operates in the 2.5–5.1 μm waveband. The IR camera has a microscopic lens with field of view 19.2 × 14.4 mm corresponding to a resolution of 0.06 mm × 0.056 mm. The focal distance between sensor and sample (corresponding to a view angle 5.5° × 4.4°) is around 230 mm. Considering, as a first approximation, the worst case of meniscus shape as a spherical cap, the interface region with a local angle less than ±60° with respect to the camera axis is about 0.85 mm. Typically a view angle not larger than 60° is sufficient to make accurate measurements neglecting the curvature (edge) effect [24]. The depth of focus is 1 mm. This would allow the measurement of the temperature profile along the entire meniscus, which was not possible with the Flir IR camera used in a previous study (Buffone and Sefiane [11]) where the depth of focus was only 100 μm. However, the better microscopic lens used in Buffone and Sefiane [11] allowed for better spatial resolution 31.25 μm compared with the 60.19 μm of the present IR camera.

In order to check the IR camera readings, we took a heated plate from below and covered the upper surface with matt black paint (to have high emissivity, above 0.95). We attached a calibrated platinum resistance temperature detector PT100 to the upper surface and compared its temperature with the IR reading for three heater power settings. The difference between IR camera and PT100 sensor readings is found to be less than 6%.

3. Results and discussion

Fig. 3 shows a horizontal diametrical optical section of the horizontally positioned tube where the liquid inside the capillary tube is shown close to the tube mouth; the meniscus curved interface is seen as well as the tracer particles used to seed the liquid. Fig. 3 is a superimposition of 20 frames to get the particle trajectories. As can be seen two convective counter rotating Marangoni rolls are present close to the meniscus interface. These are cross sections of a toroidal Marangoni roll which is driven by surface tension gradient generated by differences in temperature along the meniscus interface, as explained by Buffone and Sefiane [8]. These vortices move warmer liquid from the meniscus centre towards the wedge along the meniscus interface. For continuity then the liquid is driven back in the bulk and accelerated in the middle of the capillary tube towards the meniscus interface.

In the first experiment the spinning frequency of the Marangoni rolls is reported as a function of the heat flux. Heating loads of 0, 0.09, 0.34, 0.57, and 1.08 W where applied corresponding to 0, 10, 36, 60, and 115 kW/m^2 Fig. 4 reports the roll spinning frequency (how fast a tracer particle takes to complete a loop of the Marangoni roll) as a function of the heat flux. The maximum estimated error (at the maximum heat flux of 115 kW/m^2) in locating the position of the spinning particle around a loop is ±6%, which is determined by measuring the distance between the starting and

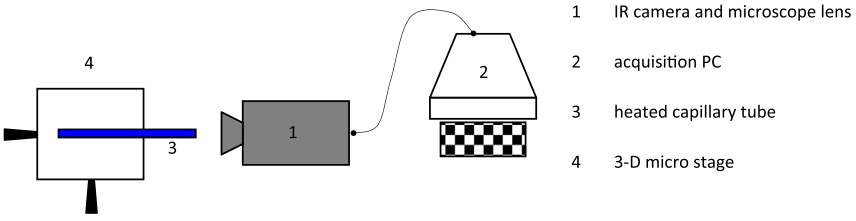

Fig. 2. Sketch of the experimental setup (top view) for IR investigation with the use of FLIR SC5000 camera.

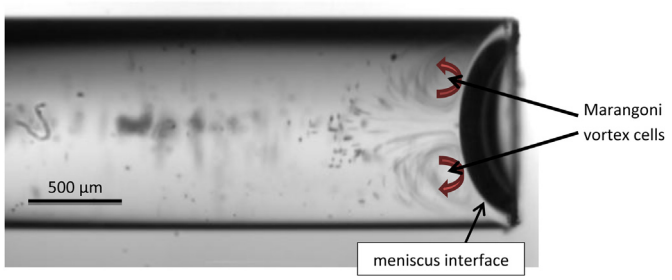

Fig. 3. Superimposition of 20 images of tracers particles. Red arrows show the direction of the Marangoni vortices optical section. (For interpretation of the references to colour in this figure legend, the reader is referred to the web version of this article.)

ending position on one loop. The results of Fig. 4 have been taken at least 1 min after imposing a given heating power. The IR temperature measurements showed that steady state was reached few seconds after each power setting. Therefore we can assume that the roll spinning frequency relates to steady state conditions. As can be seen from Fig. 4, for heat fluxes below 10 kW/m^2 there is no appreciable movement of the tracer particles. It is believed that this is due to the small temperature gradient established along the meniscus interface, as will be shown later. This produces small gradients of surface tension that are not big enough to overcome the viscosity of the silicon oil and set the particles in motion. At higher power settings the temperature gradient along the meniscus interface (as will be shown later) becomes large enough and the on-set of Marangoni convection is established. When the next power setting (1.58 W corresponding to 168 kW/m^2) was applied it was noted that the meniscus first deformed and then de-pinned from the tube mouth. The meniscus would recede inside the tube past the heater and would position several diameters far from the heater. When the heater was switched off the meniscus would rewet the capillary tube and would position again on the tube mouth. Several retests were performed and the meniscus would de-pin at the same power level. The deformation and subsequent de-pinning of the meniscus from the tube mouth might be due to thermocapillary stresses which act at the meniscus triple line, like those investigated in a meniscus formed in a heated vertical pore by Pratt and Hallinan [25]. In the present work these stresses are always present even at null heating power, because of the slight evaporation of silicon oil at ambient temperature, however they are not big enough to produce the de-pinning of the meniscus. With increasing heating at a certain power setting (1.58 W) the imposed temperature gradient at the triple line generates thermocapillary stresses high enough that first provoke the deformation of the meniscus interface and eventually its de-pinning from the tube mouth. This interesting phenomenon needs a closer examination, which is beyond the scope of the present study.

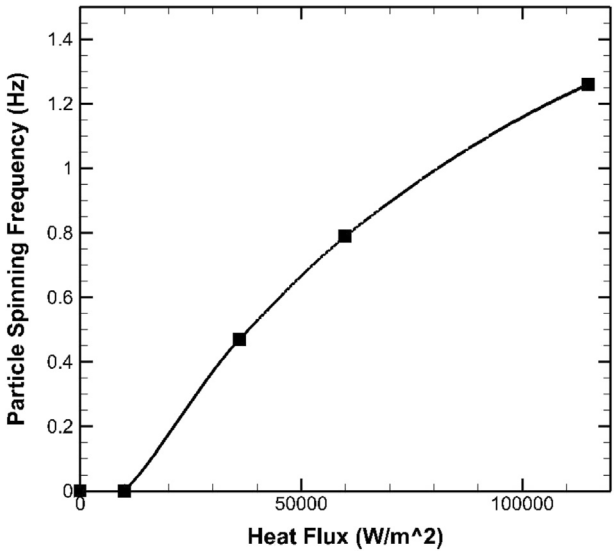

Fig. 4. Tracer particle spinning frequency as a function of electric heat flux.

In the second experiment IR measurements of the meniscus interface were carried out at the same power levels as for the Marangoni roll spinning frequency measurements. Fig. 5 reproduces on the left the temperature map of the tube mouth and on the right the temperature profile along section **A**–**B** for null applied heating power. The temperature profiles along horizontal diametrical section of the tube mouth present two minima marked by **L** and **M** which are in correspondence to the meniscus triple line region where most of the evaporation takes place and it reproduces the findings of Buffone and Sefiane [11] for evaporating alcohols. The temperature outside the minima **L** and **M** has not much meaning because first the tube wall has a different emissivity than silicon oil and then air is transparent to IR radiation. It is worth noting that the distance between minima **L** and **M** is larger than the tube ID of 1 mm. This is classical to IR measurements and is due to edge effects. Therefore the temperature gradients reported in the next Fig. 6 are lower than reality.

The temperature profiles at the tube mouth along the meniscus interface are somewhat different from the ones reported in a previous study (Buffone and Sefiane [11]). This is due to the fact that in the previous study the depth of focus of the IR camera with the microscopic lens was only 100 μm, therefore only a portion of the meniscus interface was in focus. In the present study the depth of focus is 1 mm, therefore the temperature of the whole meniscus can be measured.

Fig. 6 reports the temperature profile along the meniscus interface at tube mouth (on the left) and the temperature difference between the centre and the wedge of the meniscus (on the right) for various heat flux, with the highest heat flux just before the meniscus detaches from the tube mouth. In Fig. 6 on the left the ambient temperature has been reported by a dashed and dotted line. As seen in Fig. 6 on the left, at low heat fluxes (up to 10 kW/m^2) the liquid inside the tube is colder than the ambient. This is due to evaporative cooling effect. At larger heat fluxes the silicon oil heats up and the silicon oil becomes hotter than the ambient; but the temperature at the meniscus triple line remains always lower than the meniscus centre. It is worth noticing that the location of the maximum temperatures of the curves in Fig. 6 on the left, move outwards. This is presumably due to the borosilicate tube and its emissivity, and the 60.19 μm resolution of the IR camera. Temperature readings in this region are not accurate.

The driving force for the convection studied in the present experimental investigation is the temperature difference along the meniscus interface from the centre to the wedge. As can be seen from Fig. 6 (graph on the right), the temperature difference along the meniscus interface increases from about 0.5 °C to up to 2.2 °C at the highest heat flux. From the spinning frequency measurements of Fig. 4 and from Fig. 6, it can be said that for temperature differences below 0.64 °C (10^4 W/m^2) there is no convection; larger heat fluxes produce temperature differences big enough that set about the Marangoni convection observed.

4. Conclusions

On-set of Marangoni convection in low viscosity silicon oil inside borosilicate capillary tube of 1 mm ID is reported in the present

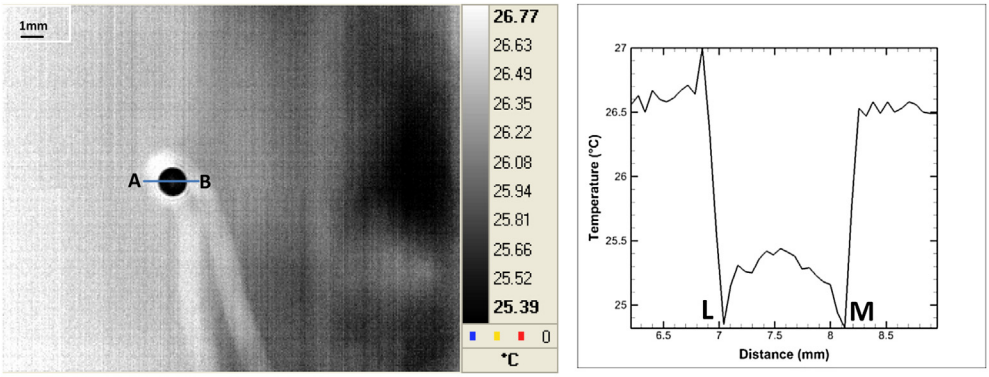

Fig. 5. IR temperature map of the tube mouth on the left and temperature profile along section **A**–**B** on the right. **L** and **M** are the temperature deeps at the meniscus triple line region inside the tube.

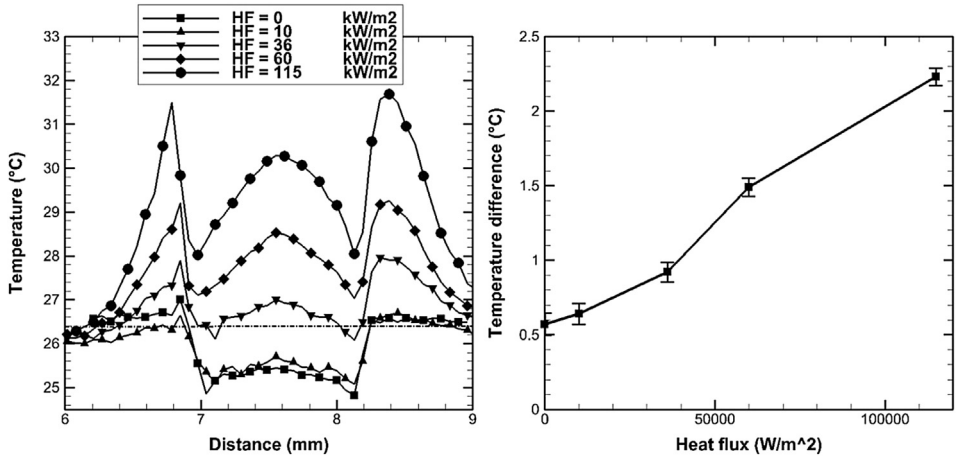

Fig. 6. IR temperature profiles of the meniscus at the tube mouth for different applied Heat Flux (HF) on the left; dashed and dotted line is the ambient temperature measured by a thermometer. Temperature differences between wedge and centre of meniscus on the right.

experimental study. The tracer particles spinning frequency is measured and the temperature profiles along the meniscus interface with the use of InfraRed thermography are reported. The tracer spinning frequency increases from 0 Hz at null power to 1.26 Hz at 115 kW/m^2. The temperature differences along the meniscus interface go from 0.57 °C at null power (due to self-induced evaporation of the silicon oil) to 2.23 °C at 115 kW/m^2. The self-induced temperature differences along the meniscus interface at low heat fluxes are found not to be big enough to set the Marangoni convection in the liquid phase. At increasing heat fluxes (36 kW/m^2) the Marangoni convection is observed and it strengthens at higher heat fluxes. At 168 kW/m^{2}it is observed that the meniscus firstly deforms considerably and then detaches from the tube mouth and recedes inside the capillary tube going to stabilize well after the electric heater. If power is removed from the electric heater, the meniscus re-wet the tube and goes to position itself again at the tube mouth.

References

[1] D. Reay, P. Kew, Heat Pipes: Theory, Design and Applications, fifth ed., Elsevier, London, 2006.
[2] S. Nebuloni, J.R. Thome, Numerical modeling of laminar annular film condensation for different channel shapes, Int. J. Heat Mass Transfer 53 (2010) 2615–2627.
[3] H.S. Wang, J.W. Rose, Film condensation in horizontal microchannels: effect of channel shape, Int. J. Therm. Sci. 45 (2006) 1205–1212.
[4] V.G.H. Frischat, K. Herr, H. Barklage-Hilgefort, Problemebei derVorbCreitung-GlastechnischerIntersuchungen in Weltraum, Glastech. Ber. 53 (1980) 1–9.
[5] D. Schwabe, Marangoni effects in crystal growth melts, Physicochem. Hydrodyn. 2 (4) (1981) 263–280.
[6] N. Ramanan, S.A. Korpela, Thermocapillary convection in an axisymmetric-pool, Comput. Fluids 18 (2) (1990) 205–215.
[7] R. Savino, in: R. Savino (Ed.), Surface Tension-driven Flows and Applications, Research Signpost, Trivandrum, Kerala, India, 2006.
[8] C. Buffone, K. Sefiane, Investigation of thermocapillary convective patterns and their role in the enhancement of evaporation from pores, Int. J. Multiphase Flow 30 (2004) 1071–1091.
[9] C. Buffone, K. Sefiane, J.R. Christy, Experimental investigation of self-induced thermocapillary convection for an evaporating meniscus in capillary tubes using micro-particle image velocimetry, Phys. Fluids 17 (2005) 052104.
[10] C. Buffone, K. Sefiane, W. Easson, Marangoni-driven instabilities of an evaporating liquid–vapor interface, Phys. Rev. E 71 (2005) 056302.
[11] C. Buffone, K. Sefiane, IR measurements of interfacial temperature during phase change in a confined environment, Exp. Therm. Fluid Sci. 29 (2004) 65–74.
[12] H.K. Dhavaleswarapu, P. Chamarthy, S.V. Garimella, J.Y. Murthy, Experimental investigation of steady buoyant thermocapillary convection near an evaporating meniscus, Phys. Fluids 19 (2007) 082103.
[13] P. Chamarthy, H.K. Dhavaleswarapu, S.V. Garimella, J.Y. Murthy, S.T. Wereley, Visualization of convection patterns near an evaporating meniscus using μPIV, Exp. Fluids 44 (2008) 431–438.
[14] G. Fabien, M. Antoni, K. Sefiane, Use of IR thermography to investigate heated droplet evaporation and contact line dynamics, Langmuir 27 (11) (2011) 6744–6752.
[15] R. Savino, D. Paterna, N. Favaloro, Buoyancy and Marangoni effects in an evaporating drop, AIAA J. Thermophys. Heat Transfer 16 (4) (2002) 562–574.
[16] R. Savino, S. Fico, Transient Marangoni convection in hanging evaporating drops, Phys. Fluids 16 (10) (2004) 3738–3754.
[17] D. Brutin, B. Sobac, F. Rigollet, C. Le Niliot, Infrared visualization of thermal motion inside a sessile drop deposited onto a heated surface, Exp. Therm. Fluid Sci. 35 (2011) 521–530.
[18] V. Ha, C.L. Lai, Onset of Marangoni instability of a two-component evaporating drop, Int. J. Heat Mass Transfer 45 (2002) 5143–5158.

[19] D. Brendan MacDonald, C.A. Ward, Onset of Marangoni convection for evaporating sessile droplets, J. Colloid Interface Sci. 383 (2012) 198–207.
[20] P. Kavehpour, B. Ovryn, G.H. McKinley, Evaporatively-driven Marangoni instabilities of volatile liquid spreading on thermally conductive substrates, Colloids Surf. A 206 (2002) 409.
[21] Z. Pan, H. Wang, Onset of Benard–Marangoni instability on a flat meniscus in a microchannel, in: ASME 2012 Third International Conference on Micro/Nanoscale Heat and Mass Transfer Atlanta, Georgia, USA, March 3–6, 2012, ISBN 978-0-7918-5477-8.
[22] Z. Pan, H. Wang, Bénard–Marangoni instability on evaporating menisci in capillary channels, Int. J. Heat Mass Transfer 63 (2013) 239–248.
[23] R. Markus, C. Willert, J. Kompenhans, Springer, London, 1998.
[24] T.Y. Cheng, D. Deng, C. Herman, Curvature effect quantification for in-vivo IR thermography, in: Int Mech Eng Congress Expo, 2012, p. 2, http://dx.doi.org/10.1115/IMECE2012-88105.
[25] D.M. Pratt, K.P. Hallinan, Thermocapillary effects on the wetting characteristics of a heated meniscus, J. Thermophys. Heat Transfer 11 (4) (1997) 519–525.